WALAILAK JOURNAL

http://wjst.wu.ac.th Applied Mathematics

Partial Slip Consequences on Peristaltic Transport of Williamson Fluid in an Asymmetric Channel

Safia AKRAM[1,*], Sohail NADEEM[2] and Anwar HUSSAIN[2]

[1]Department of Basic Sciences, MCS, National University of Sciences and Technology, Rawalpindi 46000, Pakistan
[2]Department of Mathematics, Quaid-i-Azam University, Islamabad 44000, Pakistan

([*]Corresponding author's e-mail: safia_akram@yahoo.com, safia@mcs.edu.pk)

Received: 5 November 2013, Revised: 5 February 2014, Accepted: 5 March 2014

Abstract

The present analysis deals with the peristaltic flow of a Williamson fluid model in an asymmetric channel with different wave forms under the effects of partial slip. The governing nonlinear partial differential equations, along with nonlinear partial slip boundary conditions, have been first simplified, using the assumptions of long wave length and low Reynolds number. The reduced nonlinear differential equations are then solved analytically by the regular perturbation method. The expression for pressure rise is computed numerically. At the end, the graphical behavior of velocity, pressure gradient, pressure rise, and streams functions for various values of Williamson fluid parameters are shown and discussed.

Keywords: Williamson fluid model, partial slip, peristaltic flow, asymmetric channel, analytical solution, different wave forms

Introduction

In certain situations, like blood arteries, suspensions, foams and polymer solutions, etc., the standard no slip condition is not valid. Therefore, in such situations, there may be partial slip between the fluid and the boundary. Mathematically, it is stated that the velocity of the walls is proportional to the shear stress of the fluid. Navier [1] was probably the first to use this idea to find the solution of the Navier-Stokes equation with partial slip boundary conditions. Later on, numerous researchers utilized this idea for various geometries. Mention may be made to the works of [2-7]. Only a limited attention has been focused on the study of partial slip in peristaltic flow phenomena. Peristalsis is a kind of fluid transport, induced by a progressive wave of area contraction or expansion along the walls of a distensible duct containing fluid. This transport is widely used in many physiological systems, especially in biomedical phenomena, and in many practical applications; important studies dealing with peristaltic flow problems include [8-16]. Recently, Nadeem and Akram [17] discussed the effects of partial slip on the peristaltic flow of a MHD Newtonian fluid in an asymmetric channel. Ali *et al*. [18] examined the slip effects on the peristaltic transport of MHD fluid with variable viscosity.

The Williamson fluid model, when there is partial slip at the boundary, is an important and interesting problem that has remained so far unexplored. Therefore, the aim of the present paper is to discuss the effects of partial slip on the peristaltic transport of a Williamson fluid in an asymmetric channel with different wave forms. The governing equations and partial slip conditions are simplified, using the assumptions of long wavelength and low Reynolds number. The reduced problem is then solved analytically using the regular perturbation method. The expressions for pressure rise are computed numerically. The graphical results against various physical parameters are made and discussed.

Fluid model

The balance of mass and momentum, for an incompressible fluid is given by;

$$\operatorname{div}\mathbf{V} = 0, \tag{1}$$

$$\rho\frac{d\mathbf{V}}{dt} = \operatorname{div}\mathbf{S} + \rho\mathbf{f}, \tag{2}$$

where ρ is the density, $\mathbf{V}$ is the velocity vector, $\mathbf{S}$ is the Cauchy stress tensor, $\mathbf{f}$ represents the specific body force, and d/dt represents the material time derivative. The constitutive equation for Williamson fluid is given by [19];

$$\mathbf{S} = -P\mathbf{I} + \boldsymbol{\tau}, \tag{3}$$

$$\boldsymbol{\tau} = -\left[\eta_\infty + (\eta_0 + \eta_\infty)\left(1 - \Gamma\bar{\dot{\gamma}}\right)^{-1}\right]\bar{\dot{\gamma}}, \tag{4}$$

in which $P\mathbf{I}$ is the spherical part of the stress due to constraint of incompressibility, $\boldsymbol{\tau}$ is the extra stress tensor, η_∞ is the infinite shear rate viscosity, η_0 is the zero shear rate viscosity, Γ is the time constant. and $\dot{\gamma}$ is defined as;

$$\bar{\dot{\gamma}} = \sqrt{\frac{1}{2}\sum_i\sum_j \bar{\dot{\gamma}}_{ij}\bar{\dot{\gamma}}_{ji}} = \sqrt{\frac{1}{2}\Pi}, \tag{5}$$

Here Π is the second invariant strain tensor. We consider the constitutive Eq. (4), the case for which $\eta_\infty = 0$ and $\Gamma\dot{\gamma} < 1$. The component of extra stress tensor, therefore, can be written as;

$$\bar{\boldsymbol{\tau}} = -\eta_0\left[(1 - \Gamma\bar{\dot{\gamma}})^{-1}\right]\bar{\dot{\gamma}} = -\eta_0\left[(1 + \Gamma\bar{\dot{\gamma}})\right]\bar{\dot{\gamma}}. \tag{6}$$

Mathematical formulation

Let us consider the peristaltic transport of an incompressible Williamson fluid in a two dimensional channel of width $\bar{d}_1 + \bar{d}_2$. The flow is generated by sinusoidal wave trains propagating with constant speed c along the channel walls. The geometry of the wall surface is defined as;

$$\begin{aligned} Y = H_1 &= \bar{d}_1 + \bar{a}_1\cos\left[\frac{2\pi}{\lambda}\left(\bar{X} - c\bar{t}\right)\right], \\ Y = H_2 &= -\bar{d}_2 - \bar{b}_1\cos\left[\frac{2\pi}{\lambda}\left(\bar{X} - c\bar{t}\right) + \phi\right], \end{aligned} \tag{7}$$

where $\bar{a}_1$ and $\bar{b}_1$ are the amplitudes of the waves, λ is the wave length, $\bar{d}_1 + \bar{d}_2$ is the width of the channel, c is the velocity of propagation, $\bar{t}$ is the time, and $\bar{X}$ is the direction of wave propagation. The phase difference ϕ varies in the range $0 \le \phi \le \pi$, in which $\phi = 0$ corresponds to a symmetric channel with waves out of phase, and $\phi = \pi$, in which the waves are in phase; further, $\bar{a}_1, \bar{b}_1, \bar{d}_1, \bar{d}_2$ and ϕ satisfy the condition;

$$\bar{a}_1^2 + \bar{b}_1^2 + 2\bar{a}_1\bar{b}_1 \cos\phi \le \left(\bar{d}_1 + \bar{d}_2\right)^2.$$

The equations governing the flow of a Williamson fluid are given by;

$$\frac{\partial \bar{U}}{\partial \bar{X}} + \frac{\partial \bar{V}}{\partial \bar{Y}} = 0, \tag{8}$$

$$\rho\left(\frac{\partial \bar{U}}{\partial \bar{t}} + \bar{U}\frac{\partial \bar{U}}{\partial \bar{X}} + \bar{V}\frac{\partial \bar{U}}{\partial \bar{Y}}\right) = -\frac{\partial \bar{P}}{\partial \bar{X}} - \frac{\partial \bar{\boldsymbol{\tau}}_{\bar{X}\bar{X}}}{\partial \bar{X}} - \frac{\partial \bar{\boldsymbol{\tau}}_{\bar{X}\bar{Y}}}{\partial \bar{Y}}, \tag{9}$$

$$\rho\left(\frac{\partial \bar{V}}{\partial \bar{t}} + \bar{U}\frac{\partial \bar{V}}{\partial \bar{X}} + \bar{V}\frac{\partial \bar{V}}{\partial \bar{Y}}\right) = -\frac{\partial \bar{P}}{\partial \bar{Y}} - \frac{\partial \bar{\boldsymbol{\tau}}_{\bar{X}\bar{Y}}}{\partial \bar{X}} - \frac{\partial \bar{\boldsymbol{\tau}}_{\bar{Y}\bar{Y}}}{\partial \bar{Y}}. \tag{10}$$

Introducing a wave frame $(\bar{x}, \bar{y})$ moving with velocity c away from the fixed frame $(\bar{X}, \bar{Y})$ by the transformation;

$$\bar{x} = \bar{X} - c\bar{t},\ \bar{y} = \bar{Y},\ \bar{u} = \bar{U} - c,\ \bar{\mathrm{v}} = \bar{V}\ \textit{and}\ \ \bar{P}(x) = \bar{P}(X,t), \tag{11}$$

Defining;

$$\begin{gathered} x = \frac{\bar{x}}{\lambda},\ \ y = \frac{\bar{y}}{d_1},\ \ u = \frac{\bar{u}}{c},\ \ \mathrm{v} = \frac{\bar{\mathrm{v}}}{c},\ t = \frac{c}{\lambda}\bar{t},\ \ h_1 = \frac{\bar{h}_1}{\bar{d}_1}, \\ h_2 = \frac{\bar{h}_2}{\bar{d}_2},\ \ \tau_{xx} = \frac{\lambda}{\eta_0 c}\bar{\tau}_{\bar{x}\bar{x}},\ \ \tau_{xy} = \frac{\bar{d}_1}{\eta_0 c}\bar{\tau}_{\bar{x}\bar{y}},\ \ \tau_{yy} = \frac{\bar{d}_1}{\eta_0 c}\bar{\tau}_{\bar{y}\bar{y}}, \\ \delta = \frac{\bar{d}_1}{\lambda},\ \ \mathrm{Re} = \frac{\rho c \bar{d}_1}{\eta_0},\ \ We = \frac{\Gamma c}{d_1},\ \ P = \frac{\bar{d}_1^2}{c\lambda\eta_0}\bar{P},\ \ \dot{\gamma} = \frac{\bar{\dot{\gamma}}\bar{d}_1}{c}. \end{gathered} \tag{12}$$

Using the above non-dimensional quantities and the resulting equations in terms of stream function, $\Psi(u = \frac{\partial \Psi}{\partial y},\ v = -\delta\frac{\partial \Psi}{\partial x})$ can be written as;

$$\delta\,\mathrm{Re}\left[\left(\frac{\partial \Psi}{\partial y}\frac{\partial}{\partial x} - \frac{\partial \Psi}{\partial x}\frac{\partial}{\partial y}\right)\frac{\partial \Psi}{\partial y}\right] = -\frac{\partial P}{\partial x} - \delta^2\frac{\partial \tau_{xx}}{\partial x} - \frac{\partial \tau_{xy}}{\partial y}, \tag{13}$$

$$-\delta^3\,\mathrm{Re}\left[\left(\frac{\partial \Psi}{\partial y}\frac{\partial}{\partial x} - \frac{\partial \Psi}{\partial x}\frac{\partial}{\partial y}\right)\frac{\partial \Psi}{\partial x}\right] = -\frac{\partial P}{\partial y} - \delta^2\frac{\partial \tau_{xy}}{\partial x} - \delta\frac{\partial \tau_{yy}}{\partial y}, \tag{14}$$

where

$$\tau_{xx} = -2[1+We\dot{\gamma}]\frac{\partial^2\Psi}{\partial x\partial y},$$
$$\tau_{xy} = -[1+We\dot{\gamma}]\left(\frac{\partial^2\Psi}{\partial y^2} - \delta^2\frac{\partial^2\Psi}{\partial x^2}\right),$$
$$\tau_{yy} = 2\delta[1+We\dot{\gamma}]\frac{\partial^2\Psi}{\partial x\partial y},$$
$$\dot{\gamma} = \left[2\delta^2\left(\frac{\partial^2\Psi}{\partial x\partial y}\right)^2 + \left(\frac{\partial^2\Psi}{\partial y^2} - \delta^2\frac{\partial^2\Psi}{\partial x^2}\right)^2 + 2\delta^2\left(\frac{\partial^2\Psi}{\partial x\partial y}\right)^2\right]^{1/2},$$

in which δ, Re, We represent the wave, Reynolds and Weissenberg numbers, respectively. Under the assumptions of long wavelength $\delta << 1$ and low Reynolds number, and neglecting the terms of order δ and higher, Eqs. (13) and (14) take the form;

$$\frac{\partial P}{\partial x} = \frac{\partial}{\partial y}\left[1+We\frac{\partial^2\Psi}{\partial y^2}\right]\frac{\partial^2\Psi}{\partial y^2}, \tag{15}$$
$$\frac{\partial P}{\partial y} = 0. \tag{16}$$

Elimination of pressure from Eqs. (15) and (16) yields;

$$\frac{\partial^2}{\partial y^2}\left[1+We\frac{\partial^2\Psi}{\partial y^2}\right]\frac{\partial^2\Psi}{\partial y^2} = 0. \tag{17}$$

The dimensionless mean flow Q is defined by;

$$Q = F + 1 + d, \tag{18}$$

in which;

$$F = \int_{h_2(x)}^{h_1(x)}\frac{\partial\Psi}{\partial y}dy = \Psi(h_1(x) - h_2(x)), \tag{19}$$

where

$$h_1(x) = 1 + a\cos 2\pi x, h_2(x) = -d - b\cos(2\pi x + \phi). \tag{20}$$

The boundary conditions in terms of stream function Ψ are defined as;

$$\Psi = \frac{F}{2}, \quad \frac{\partial \Psi}{\partial y} = -\beta \tau_{xy} - 1 \quad at \quad y = h_1(x),$$
$$\Psi = -\frac{F}{2}, \quad \frac{\partial \Psi}{\partial y} = \beta \tau_{xy} - 1 \text{ at } \quad y = h_2(x). \tag{21}$$

In the above conditions, $\beta = 0$ corresponds to the no slip conditions.

Exact solution

The exact solution of Eq. (17) is obtained as follows;

$$\frac{\partial^2 \Psi}{\partial y^2} = T \tag{21a}$$

so Eq. (17) can be written as;

$$\frac{\partial^2}{\partial y^2}(1 + WeT)T = 0.$$

The twice integration of the above equation yields;

$$WeT^2 + T = A + By.$$

The roots of above equation are;

$$T = \frac{-1 \pm \sqrt{1 + 4(A + By)We}}{2We}. \tag{21b}$$

With the help of (21a) and (21b), we can write;

$$\frac{\partial^2 \Psi}{\partial y^2} = \frac{-1 \pm \sqrt{1 + 4(A + By)We}}{2We}.$$

which after twice integrating gives;

$$\Psi = -\frac{y^2}{4We} \pm \frac{(1 + 4(A + By)We)^{5/2}}{60B^2We^2} + T_1 y + T_2,$$

in which the constant appearing in the above equation can be calculated using boundary conditions. However, to compute these constants exactly seems to be very difficult; either we can calculate approximately, or we can find the solution of the given equation analytically.

Perturbation solution

Since Eq. (17) is a nonlinear equation, we employ the regular perturbation method to find the analytical solution.
For the perturbation solution, we expand Ψ, F and P as;

$$\Psi = \Psi_0 + We\Psi_1 + O(We^2), \tag{22}$$

$$F = F_0 + WeF_1 + O(We^2), \tag{23}$$

$$P = P_0 + WeP_1 + O(We^2). \tag{24}$$

Substituting the above expressions in Eqs. (15) and (17) and boundary conditions (21), we get the following system.

System of order We^0

$$\frac{\partial^4 \Psi_0}{\partial y^4} = 0, \tag{25}$$

$$\frac{\partial P_0}{\partial x} = \frac{\partial^3 \Psi_0}{\partial y^3}, \tag{26}$$

$$\Psi_0 = \frac{F_0}{2}, \quad \frac{\partial \Psi_0}{\partial y} = \beta \frac{\partial^2 \Psi_0}{\partial y^2} - 1 \quad on \quad y = h_1(x), \tag{27}$$

$$\Psi_0 = -\frac{F_0}{2}, \quad \frac{\partial \Psi_0}{\partial y} = -\beta \frac{\partial^2 \Psi_0}{\partial y^2} - 1 \quad on \quad y = h_2(x). \tag{28}$$

System of order We^1

$$\frac{\partial^4 \Psi_1}{\partial y^4} = -\frac{\partial^2}{\partial y^2}\left(\frac{\partial^2 \Psi_0}{\partial y^2}\right)^2, \tag{29}$$

$$\frac{\partial P_1}{\partial x} = \frac{\partial^3 \Psi_1}{\partial y^3} + \frac{\partial}{\partial y}\left(\frac{\partial^2 \Psi_0}{\partial y^2}\right)^2, \tag{30}$$

$$\Psi_1 = \frac{F_1}{2}, \quad \frac{\partial \Psi_1}{\partial y} = \beta\left(\frac{\partial^2 \Psi_1}{\partial y^2} + \left(\frac{\partial^2 \Psi_0}{\partial y^2}\right)^2\right) \quad on \quad y = h_1(x), \tag{31}$$

$$\Psi_1 = -\frac{F_1}{2}, \quad \frac{\partial \Psi_1}{\partial y} = -\beta\left(\frac{\partial^2 \Psi_1}{\partial y^2} + \left(\frac{\partial^2 \Psi_0}{\partial y^2}\right)^2\right) \quad on \quad y = h_2(x). \tag{32}$$

Solution for system of order We^0

The solution of Eq. (25) satisfying the boundary conditions (27) and (28) can be written as;

$$\Psi_0 = C_0 + C_1 y + C_2 \frac{y^2}{2!} + C_3 \frac{y^3}{3!}, \tag{33}$$

where

$$C_0 = -\left(\frac{F_0(h_1 + h_2)(h_1^2 - 4h_1h_2 + h_2^2) - (h_1^2 - h_2^2)2(3F_0\beta + h_1h_2)}{2(h_1 - h_2)^2(h_1 - h_2 - 6\beta)} \right),$$

$$C_1 = -\left(\frac{h_1^3 - h_2^3 + 6F_0h_1h_2 + 3h_1h_2(h_1 - h_2) + 6F_0\beta(h_1 - h_2)}{(h_1 - h_2)^2(h_1 - h_2 - 6\beta)} \right), \tag{34}$$

$$C_2 = \frac{6(F_0 + h_1 - h_2)(h_1 + h_2)}{(h_1 - h_2)^2(h_1 - h_2 - 6\beta)}, \qquad C_3 = -\left(\frac{12(F_0 + h_1 - h_2)}{(h_1 - h_2)^2(h_1 - h_2 - 6\beta)} \right).$$

The axial pressure gradient at this order is;

$$\frac{dP_0}{dx} = -\left(\frac{12(F_0 + h_1 - h_2)}{(h_1 - h_2)^2(h_1 - h_2 - 6\beta)} \right). \tag{35}$$

For one wavelength, the integration of Eq. (35), yields;

$$\Delta P_0 = \int_0^1 \frac{dP_0}{dx}\, dx. \tag{36}$$

The above solution is for viscous fluid, which agrees with the results obtained by [20] in the absence of slip parameter.

Solution for system of order We^1

Substituting the zeroth-order solution (33) into (29), the solution of the resulting problem satisfying the boundary conditions take the following form;

$$\Psi_1 = C_4 \frac{y^3}{3!} + C_5 \frac{y^2}{2!} + C_6 y + C_7 - C_3^2 \frac{y^4}{12}, \tag{37}$$

where

$$C_4 = 2\left(\frac{-6F_1(h_1 - h_2)^3(-h_1 + h_2 + 6\beta)^2 + 144(F_0 + h_1 - h_2)^2\left(h_1^3 - 3h_1^2\beta + h_2^2(h_2 + 3\beta)\right)}{(h_1 - h_2)^5(h_1 - h_2 - 6\beta)(-h_1 + h_2 + 6\beta)^2} \right),$$

$$C_5 = \frac{1}{3(h_1-h_2)^2(h_1-h_2-6\beta)(h_1-h_2-2\beta)}\Bigg) 18F_1(h_1+h_2)(h_1-h_2-2\beta)$$

$$+\frac{72(F_0+h_1-h_2)^2}{(h_1-h_2)^3(-h_1+h_2+6\beta)^2}\Bigg) -4(h_1-h_2)\left(h_1^4+2h_1^3h_2+2h_1h_2^3+h_2^4\right)$$

$$+3\beta\left(5h_1^4+8h_1^3h_2-10h_1^2h_2^2+8h_1h_2^3+5h_2^4\right)-18\beta^2(h_1-h_2)(h_1+h_2)^2\Bigg)\Bigg),$$

$$C_6 = \frac{1}{3(h_1-h_2)^2(h_1-h_2-6\beta)(h_1-h_2-2\beta)}$$

$$\left(\left(\frac{36(F_0+h_1-h_2)^2(h_1+h_2)\left(4h_1h_2(h_1-h_2)\left(2h_1^2-h_1h_2+2h_2^2\right)-6(h_1-h_2)^3\beta^2\right)}{(h_1-h_2)^3(-h_1+h_2+6\beta)^2-18F_1(h_1-h_2-2\beta)(-h_2\beta+h_1(h_2+\beta))}\right)\right.$$

$$\left.+\left(\frac{\beta\left(5h_1^4-36h_1^3h_2+38h_1^2h_2^2-36h_1h_2^3+5h_2^4\right)}{(h_1-h_2)^3(-h_1+h_2+6\beta)^2-18F_1(h_1-h_2-2\beta)(-h_2\beta+h_1(h_2+\beta))}\right)\right),$$

$$C_7 = \frac{1}{12(h_1-h_2)^2(h_1-h_2-6\beta)(h_1-h_2-2\beta)}\Bigg) -6F_1(h_1+h_2)(h_1-h_2-2\beta)$$

$$\left(h_1^2-4h_1h_2+h_2^2-6\beta(h_1-h_2)\right)$$

$$+\left(\frac{144h_1(F_0+h_1-h_2)^2\left(h_1(h_1-h_2)\left(h_1^4-2h_1^3h_2-3h_1^2h_2^2-4h_2^4\right)\right)}{(h_1-h_2)^3(-h_1+h_2+6\beta)^2}\right)$$

$$-\left(\frac{144h_1(F_0+h_1-h_2)^2\beta\left(8h_1^5-11h_1^4h_2-8h_1^3h_2^2+6h_1^2h_2^3-16h_1h_2^4+5h_2^5\right)}{(h_1-h_2)^3(-h_1+h_2+6\beta)^2}\right)$$

$$+\left(\frac{864h_1\beta^2(F_0+h_1-h_2)^2(h_1-h_2)(2h_1+h_2)\left(h_1^2+h_2^2\right)}{(h_1-h_2)^3(-h_1+h_2+6\beta)^2}\right)\Bigg). \tag{38}$$

The axial pressure gradient at this order is;

$$\frac{dP_1}{dx}=\frac{2}{\left(h_1-h_2\right)^2\left(h_1-h_2-6\beta\right)}\Bigg)-6F_1+\frac{144\left(F_0+h_1-h_2\right)^2\left(h_1^3-3h_1^2\beta+h_2^2\left(h_2+3\beta\right)\right)}{\left(h_1-h_2\right)^3\left(-h_1+h_2+6\beta\right)^2}\Bigg) \\ -\frac{144\left(F_0+h_1-h_2\right)^2\left(h_1+h_2\right)}{\left(h_1-h_2\right)^4\left(h_1-h_2-6\beta\right)^2}. \tag{39}$$

Integrating the above equation over one wavelength, we get;

$$\Delta P_1=\int_0^1\frac{dP_1}{dx}dx. \tag{40}$$

Summarizing the perturbation results for the small parameter *We*, the expression for stream functions and pressure gradient can be written as;

$$\Psi=C_0+C_1y+C_2\frac{y^2}{2}+C_3\frac{y^3}{3}+We\left(C_4\frac{y^3}{3!}+C_5\frac{y^2}{2!}+C_6y+C_7-C_3^2\frac{y^4}{12}\right) \tag{41}$$

$$\frac{dP}{dx}=-\frac{12\left(F+h_1-h_2\right)}{\left(h_1-h_2\right)^2\left(h_1-h_2-6\beta\right)}+We\left(\frac{288\left(F+h_1-h_2\right)^2\left(h_1^3-3h_1^2\beta+h_2^2\left(h_2+3\beta\right)\right)}{\left(h_1-h_2\right)^5\left(-h_1+h_2+6\beta\right)^2\left(h_1-h_2-6\beta\right)}\right. \\ \left.-\frac{144\left(F+h_1-h_2\right)^2\left(h_1+h_2\right)}{\left(h_1-h_2\right)^4\left(h_1-h_2-6\beta\right)^2}\right), \tag{42}$$

The non-dimensional pressure rise over one wavelength ΔP for the axial velocity is;

$$\Delta P=\int_0^1\frac{dP}{dx}dx. \tag{43}$$

where Cs are defined in Eqs. (34) and (38), and $\frac{dP}{dx}$ is defined in Eq. (42).

Expressions for different wave shape

The non-dimensional expressions for three considered wave forms are given as;

1) Sinusoidal wave;

$$h_1(x)=1+a\sin 2\pi x,\quad h_2(x)=-d-b\sin(2\pi x+\phi).$$

2) Triangular wave;

$$h_1(x) = 1 + a\left[\frac{8}{\pi^3}\sum_{m=1}^{\infty}\frac{(-1)^{m+1}}{(2m-1)^2}\sin(2\pi(2m-1)x)\right],$$

$$h_2(x) = -d - b\left[\frac{8}{\pi^3}\sum_{m=1}^{\infty}\frac{(-1)^{m+1}}{(2m-1)^2}\sin(2\pi(2m-1)x+\phi)\right].$$

3) Trapezoidal wave;

$$h_1(x) = 1 + a\left[\frac{32}{\pi^2}\sum_{m=1}^{\infty}\frac{\sin\frac{\pi}{8}(2m-1)}{(2m-1)^2}\sin(2\pi(2m-1)x)\right],$$

$$h_2(x) = -d - b\left[\frac{32}{\pi^2}\sum_{m=1}^{\infty}\frac{\sin\frac{\pi}{8}(2m-1)}{(2m-1)^2}\sin(2\pi(2m-1)x+\phi)\right].$$

Results and discussion

In this section, the graphical results of the problem under consideration are displayed, to see the behavior of various physical parameters of interest. **Figures 1 - 5** are prepared for pressure rise against volume flow rate Q. It is observed from **Figure 1** that, in the adverse pressure gradient ($\Delta P > 0$, in pumping region) and favorable pressure gradient ($\Delta P < 0$, in pumping region), the pressure rise decreases with the increase in Weissenberg number. From **Figures 2 - 4** it is observed that, in the adverse pressure gradient ($\Delta P > 0$, in pumping region), the pressure gradient increases with the increase in slip parameter β and amplitude of wave a and b, while in the copumping region ($\Delta P < 0$, in favorable pressure gradient), the behavior is quite opposite. In this region, the pressure rise decreases with the increase in slip parameter β and amplitude of wave a and b. It is shown in **Figure 5** that, in the adverse pressure gradient ($\Delta P > 0$, in pumping region), the pressure gradient decreases with the increase in width of the channel d, while in the free pumping ($\Delta P = 0$) and copumping region ($\Delta P < 0$, in favorable pressure gradient) the pressure rise increases with the increase in d. **Figures 6 - 9** are prepared to distinguish the behavior of pressure gradient for different values of Weissenberg number We, width of channel d, slip parameter β, and amplitude of wave a. It is observed that pressure gradient decreases with the increase of We and d (see **Figures 6** and **7**). However, it is observed from **Figures 8** and **9** that, with the increase in β and a, the pressure gradient increases in the region $x\varepsilon\,[0.2, 0.8]$. The velocity field for various values of We, β and Q are plotted in **Figures 10 - 12**. The velocity field u for different values of We are plotted in **Figure 10**. It is observed that, for positive values of y, the velocity field increases with the increase in We and, for negative values of y, velocity u has the opposite results. It is observed from **Figure 11** that, due to slip parameterβ, the velocity near the channel walls are not same, but it slips, and, also, the velocity increases with the increase in β. It is also observed from **Figure 12** that the velocity profile decreases with the increase in volume flow rate Q. The pressure rise against the volume flow rate Q for different wave shapes are shown in **Figure 13**. It is depicted that the pressure rise for the trapezoidal wave is greater than the sinusoidal wave, and the sinusoidal wave is greater than the triangular wave.

The trapping phenomena for different values of Weissenberg number We, slip parameter β, volume flow rate Q, and different wave forms are shown in **Figures 14 - 17**. It is seen from **Figures 14** that the size of the trapping bolus increases with the increase in Weissenberg number We in the upper and lower half of the channel. From **Figure 15**, it is observed that, with the increase in the values of slip parameter β, the size and number of the trapping bolus increases in the upper half of the channel, while in the lower half, the size of the trapping bolus decreases. It is depicted in **Figure 16** that the number and size of the trapping bolus reduces in the upper half of the channel, while in the lower half, the size of the trapping bolus increases with the increase of volume flow rate Q. The stream lines for three different wave shapes, trapezoidal, sinusoidal, and triangular, are shown in **Figures 17(a) - 17(c)**. The stream lines represent the particular shape of the wave which we have considered.

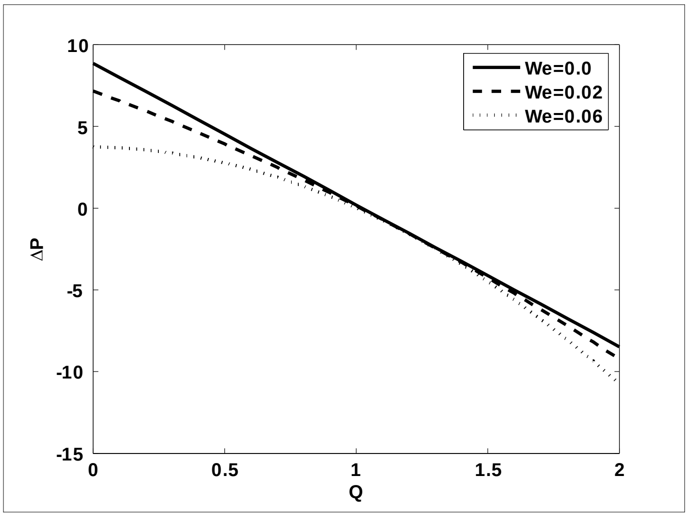

Figure 1 Variation of ΔP with Q for different values of We. The other parameters are $a = 0.8$, $b = 0.5$, $d = 1$, $\phi = \frac{\pi}{6}$, $\beta = 0.04$.

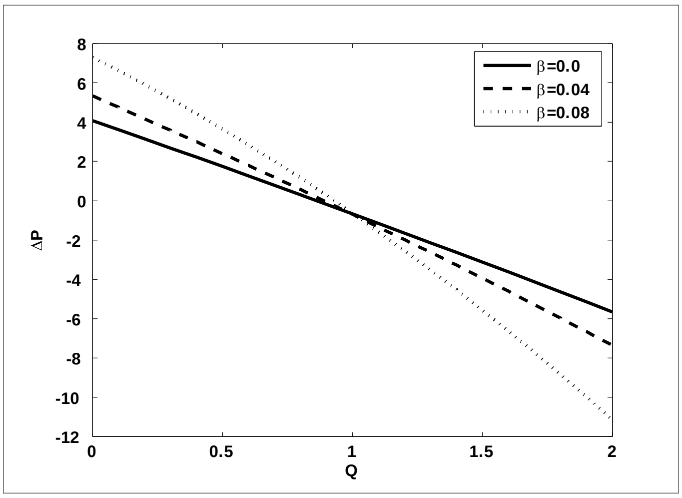

Figure 2 Variation of ΔP with Q for different values of β. The other parameters are $a = 0.7$, $b = 0.5$, $d = 1$, $\phi = \frac{\pi}{6}$, $We = 0.02$.

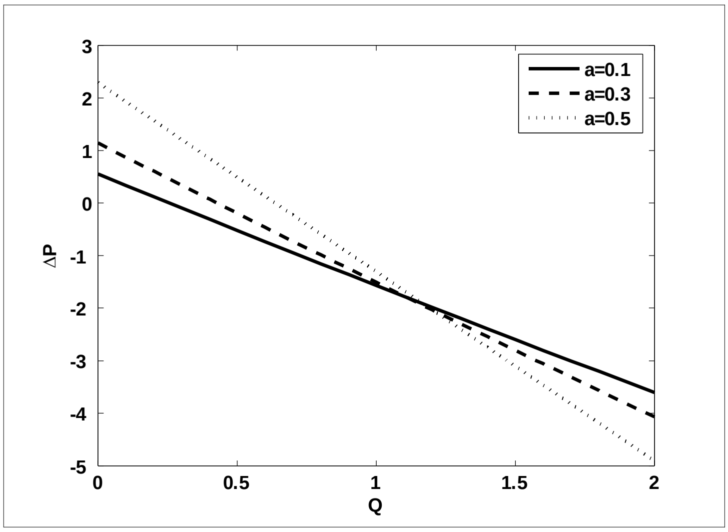

Figure 3 Variation of ΔP with Q for different values of a. The other parameters are $We = 0.04$, $b = 0.5$, $d = 1$, $\phi = \frac{\pi}{6}$, $\beta = 0.02$.

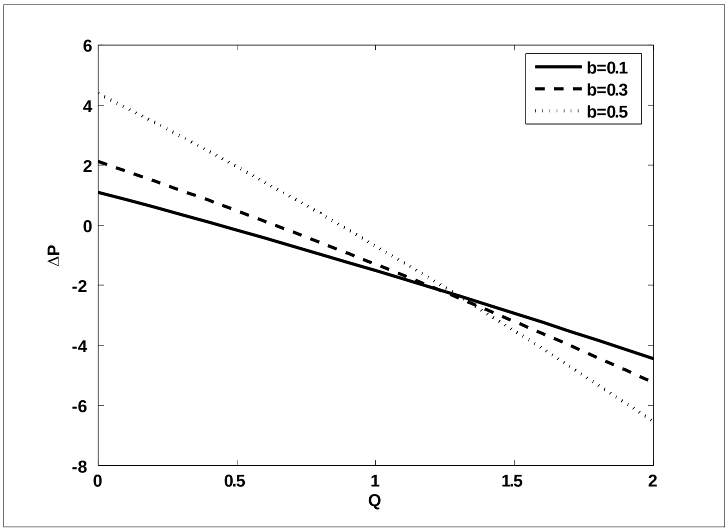

Figure 4 Variation of ΔP with Q for different values of b. The other parameters are $a = 0.7$, $We = 0.04$, $d = 1$, $\phi = \frac{\pi}{6}$, $\beta = 0.02$.

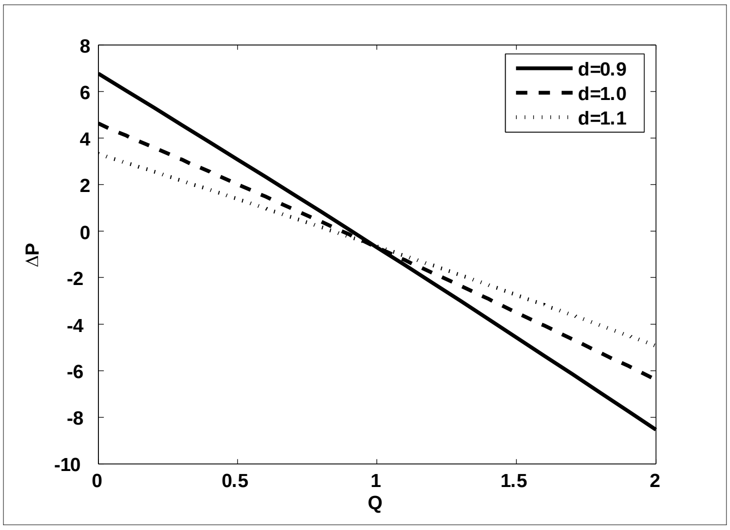

Figure 5 Variation of ΔP with Q for different values of d. The other parameters are $a = 0.7,$ $b = 0.5,$ $We = 0.02,$ $\phi = \frac{\pi}{6},$ $\beta = 0.02.$

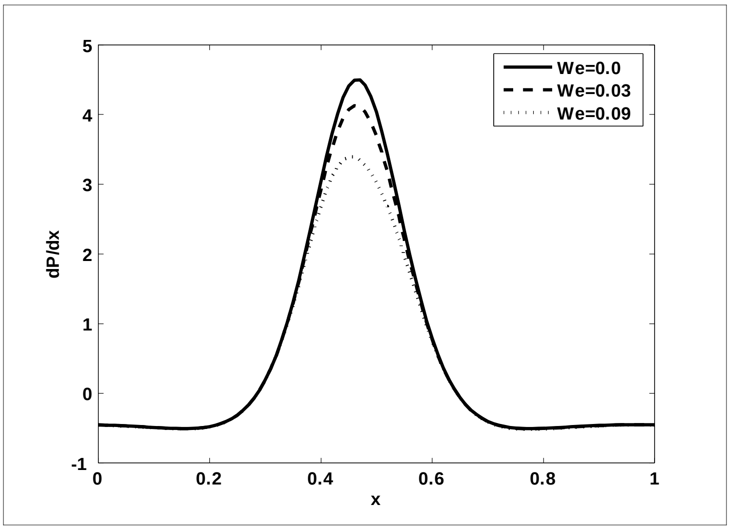

Figure 6 Variation of dP/dx with x for different values of $We.$ The other parameters are $a = 0.7,$ $b = 0.5,$ $d = 1.5,$ $\phi = \frac{\pi}{6},$ $Q = 0.5,$ $\beta = 0.06.$

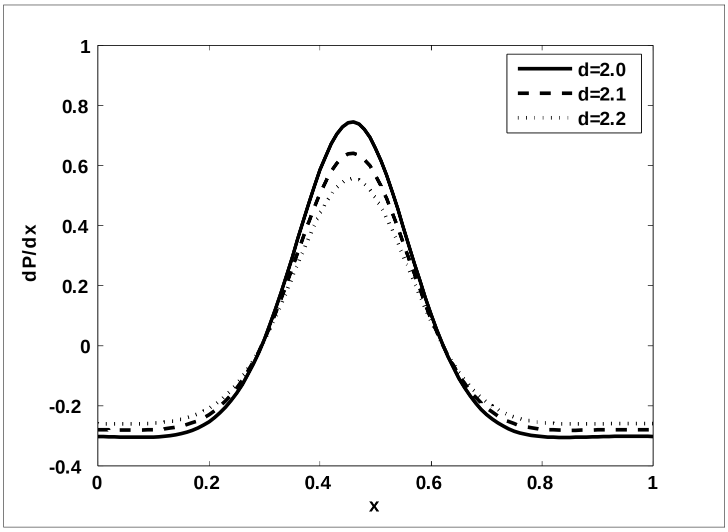

Figure 7 Variation of dP/dx with x for different values of d. The other parameters are $a=0.5$, $b=0.5$, $We=0.02$, $\phi=\frac{\pi}{6}$, $Q=0.5$, $\beta=0.04$.

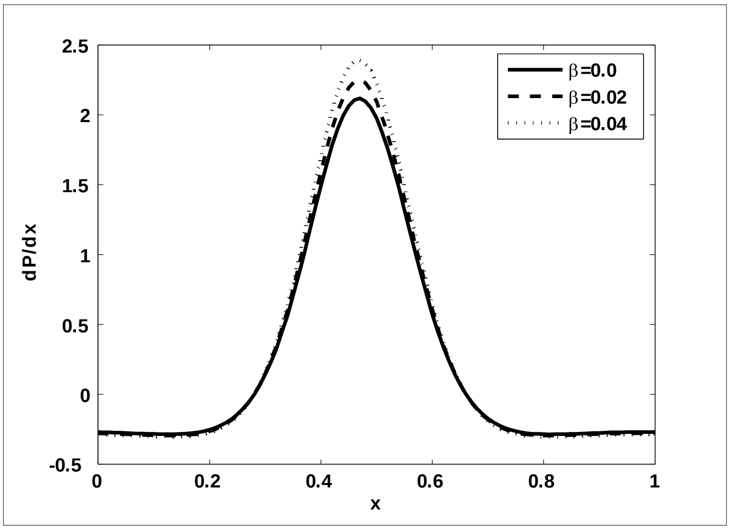

Figure 8 Variation of dP/dx with x for different values of β. The other parameters are $a=0.9$, $b=0.5$, $d=2$, $\phi=\frac{\pi}{6}$, $Q=0.5$, $We=0.03$.

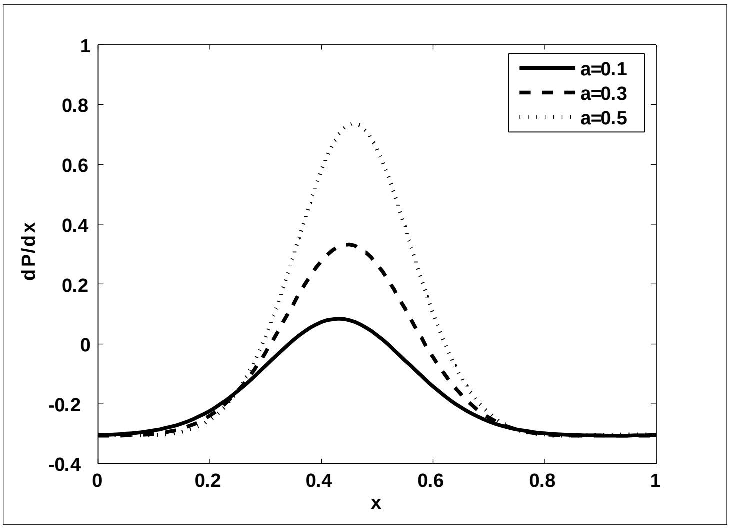

Figure 9 Variation of dP/dx with x for different values of a. The other parameters are $We = 0.0.04,\ b = 0.5,\ d = 2,\ \phi = \frac{\pi}{6},\ Q = 0.5,\ \beta = 0.04.$

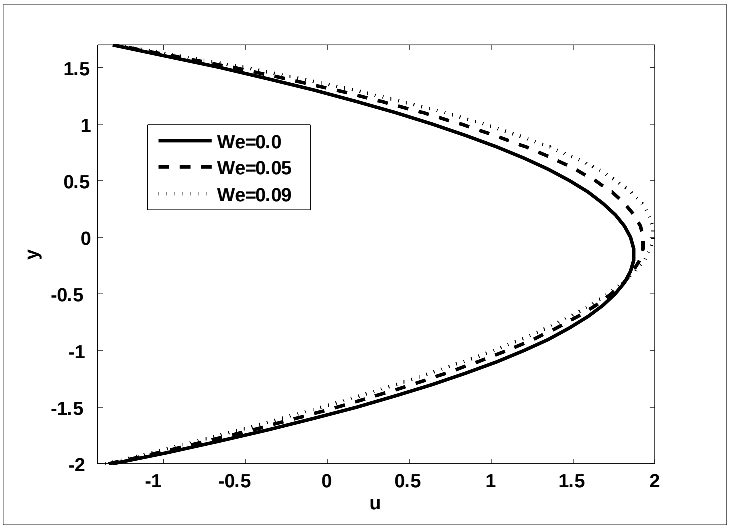

Figure 10 Velocity profile for different values of We. The other parameters are $a = 0.7,\ b = 1.2,$ $d = 2,\ \phi = \frac{\pi}{2},\ Q = 3,\ \beta = 0.09.$

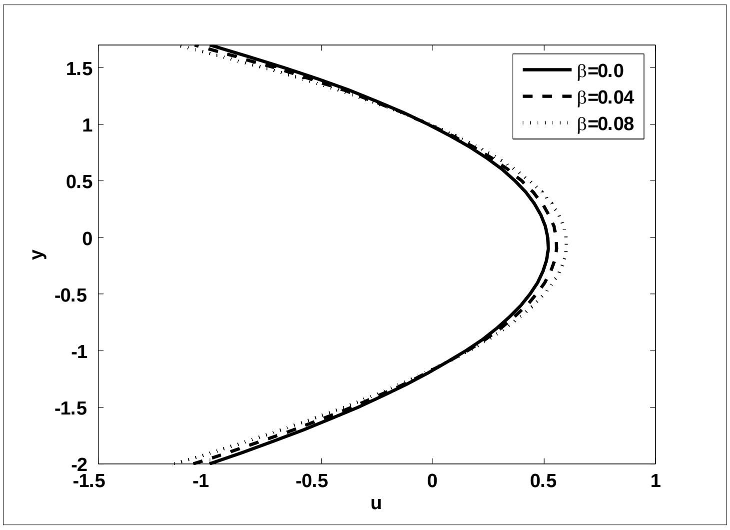

Figure 11 Velocity profile for different values of β. The other parameters are $a = 0.7,\ \ b = 1.2,$ $d = 2,\ \ \phi = \frac{\pi}{2},\ \ Q = 3,\ \ We = 0.06.$

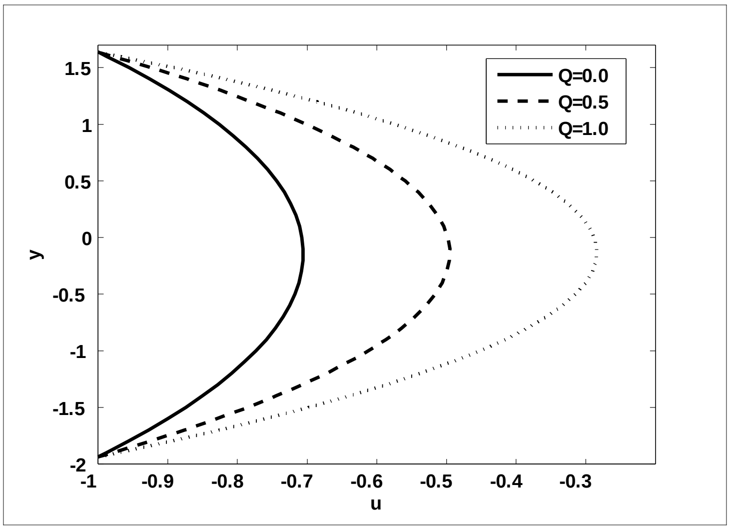

Figure 12 Velocity profile for different values of Q. The other parameters are $a = 0.7,\ \ b = 1.2,$ $d = 2,\ \ \phi = \frac{\pi}{2},\ \ We = 0.04,\ \ \beta = 0.06.$

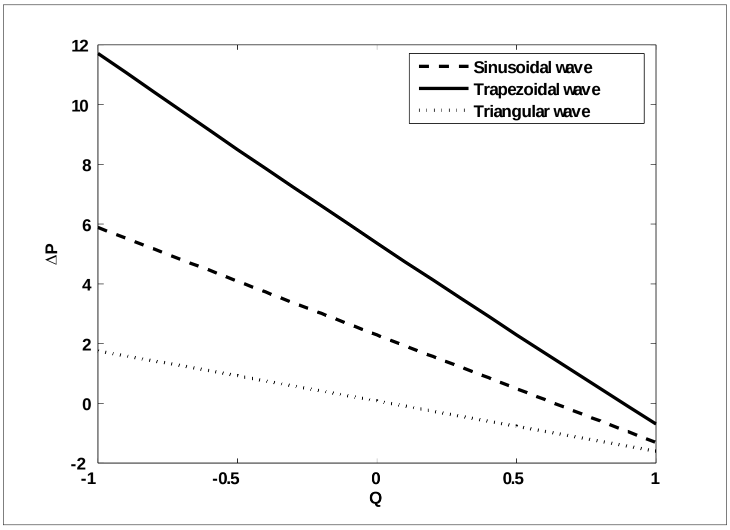

Figure 13 Variation of ΔP with Q for different wave forms. The other parameters are $a = 0.5$, $b = 0.5$, $We = 0.04$, $d = 1$, $\phi = \frac{\pi}{6}$, $\beta = 0.02$.

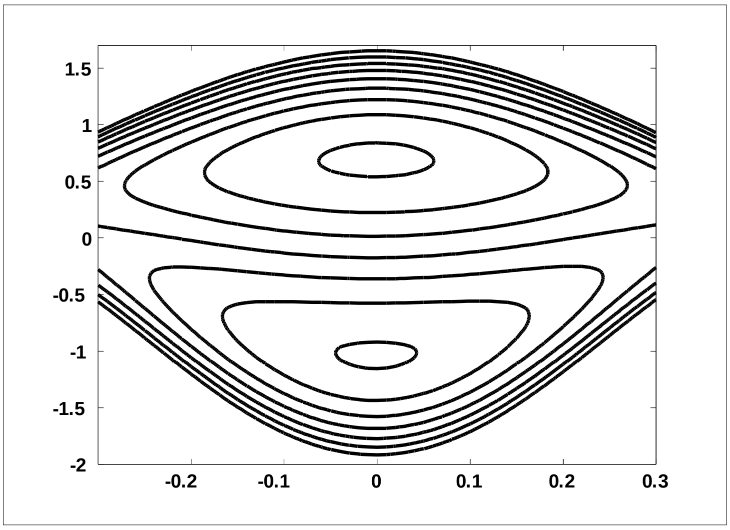

(a)

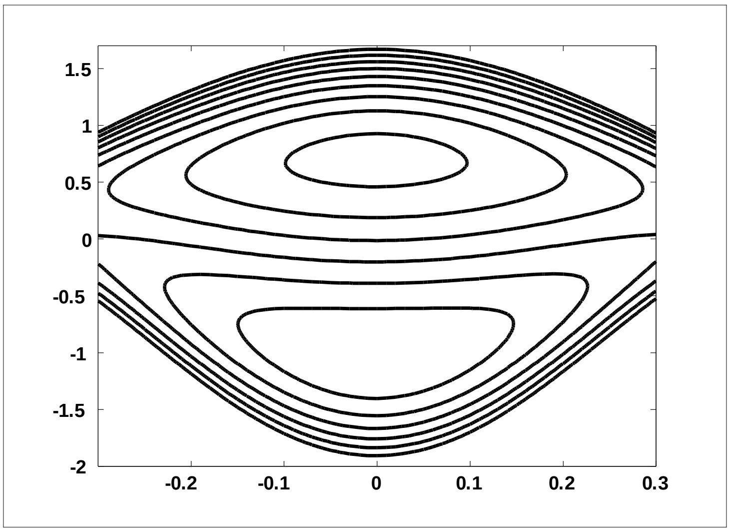

(b)

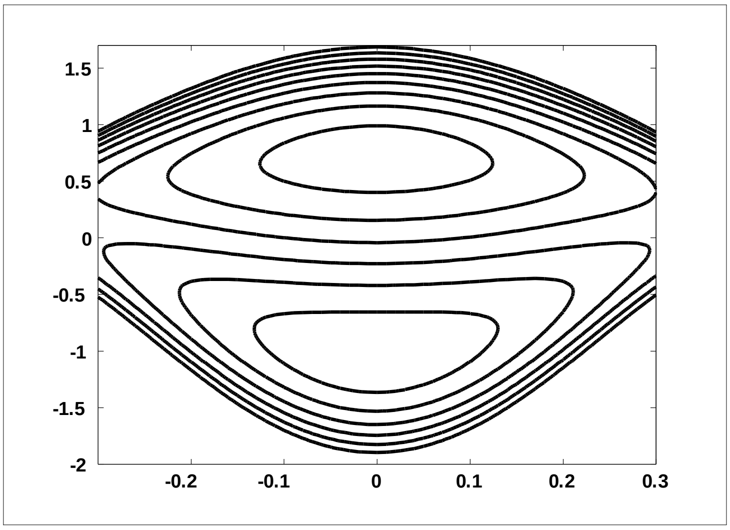

(c)

Figure 14 Stream lines for different values of We. (a) for $We = 0.04,$ (b) for $We = 0.05$ and (c) for $We = 0.06.$ The other parameters are $\phi = 0.01,\ Q = 1.5,\ a = 0.5,\ d = 0.9,\ b = 1.0,\ \beta = 0.06.$

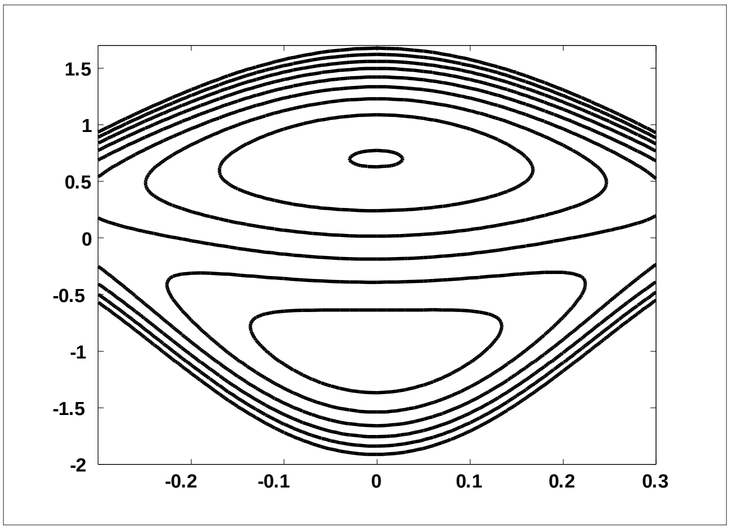

(a)

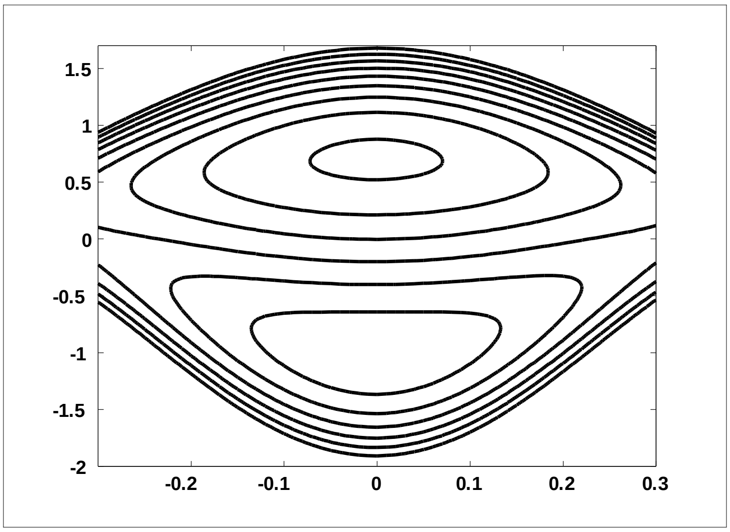

(b)

Figure 15 Stream lines for different values of β. (a) for $\beta = 0.03$ and (b) for $\beta = 0.04$. The other parameters are $\phi = 0.01,\ Q = 1.5,\ a = 0.5,\ d = 0.9,\ b = 1.0,\ We = 0.06.$

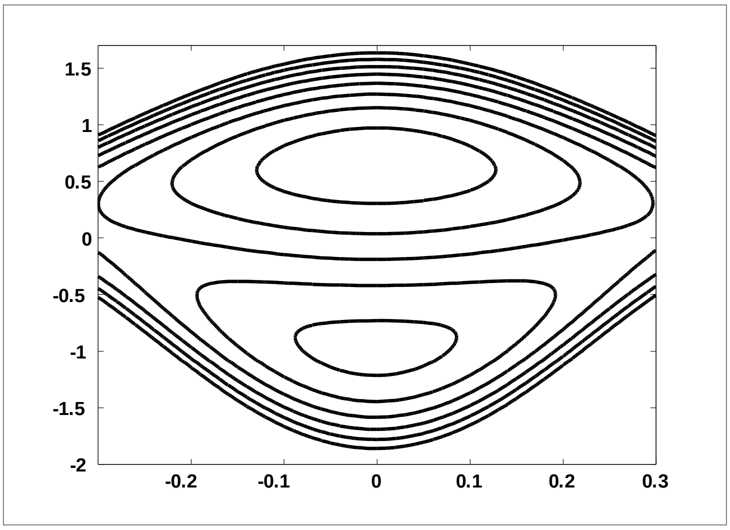

(a)

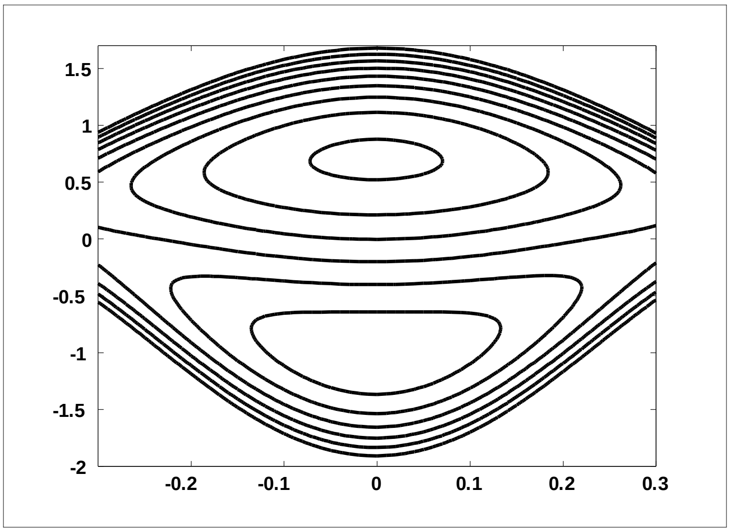

(b)

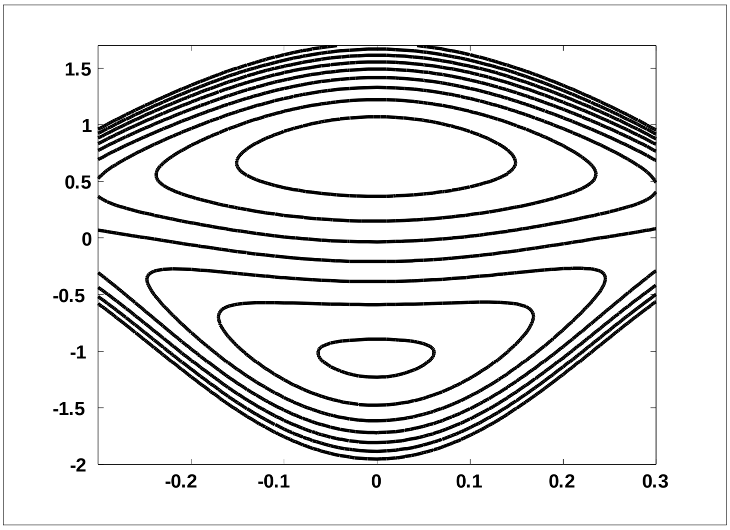

(c)

Figure 16 Stream lines for different values of Q. (a) for $Q = 1.4$, (b) for $Q = 1.5$ and (c) for $Q = 1.6$. The other parameters are $\phi = 0.01$, $We = 0.06$, $a = 0.5$, $d = 0.9$, $b = 1.0$, $\beta = 0.06$.

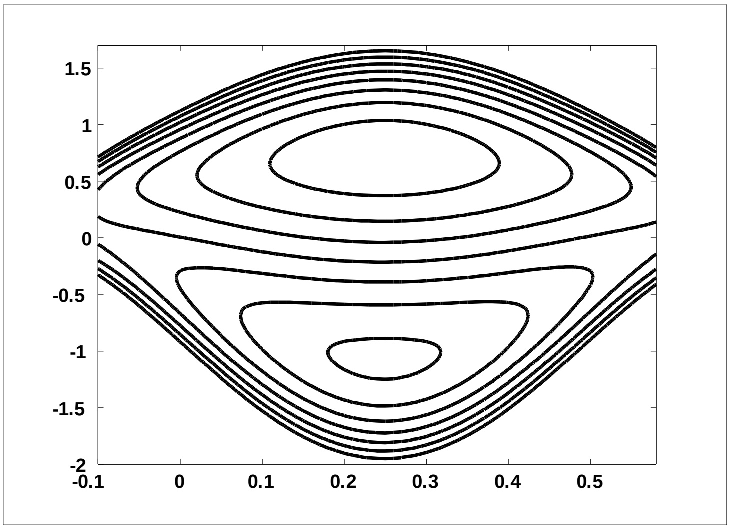

(a)

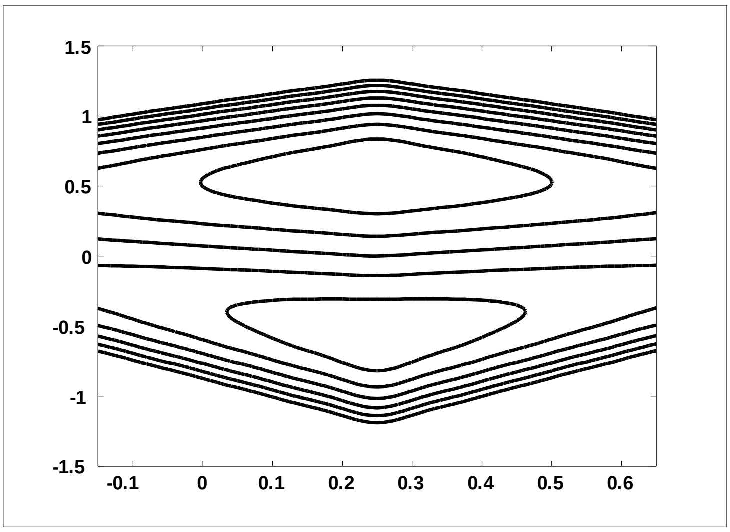

(b)

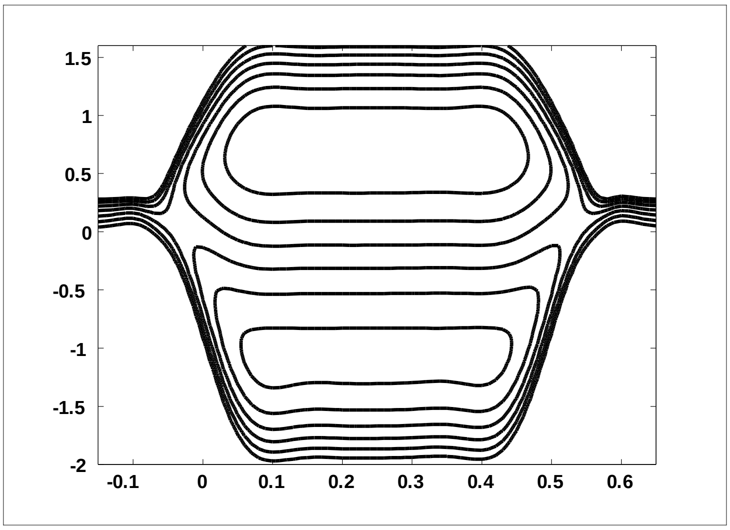

(c)

Figure 17 Stream lines for different wave forms; (a) for Sinusoidal wave, (b) Triangular wave and (c) for Trapezoidal wave. The other parameters are $\phi = 0.01$, $We = 0.04$, $Q = 1.6$, $a = 0.5$, $d = 0.9$, $b = 1.0$, $\beta = 0.04$.

Concluding remarks

This paper presents partial slip consequences on peristaltic transport of Williamson fluid in an asymmetric channel. The governing two dimensional equations have been modeled and then simplified using long wave length approximation. The results are discussed through graphs. The main finding can be summarized as follows:

1) It is observed that in the adverse pressure gradient ($\Delta P > 0$, in pumping region), the pressure gradient increases with the increase in slip parameterβ, and amplitude of wave a and b, while in the copumping region, the behavior is quite opposite.

2) The pressure gradient decreases with the increase in width of the channel d, in the adverse pressure gradient, while in the free pumping ($\Delta P = 0$) and copumping region ($\Delta P < 0$, in favorable pressure gradient), the behavior is quite opposite.

3) The velocity profile decreases with the increase in volume flow rate Q.

4) The pressure rise for the trapezoidal wave is greater than the sinusoidal wave, and the sinusoidal wave is greater than the triangular wave.

5) The size of the trapping bolus increases with an increase in Weissenberg number We in the upper and lower half of the channel.

6) The size and number of the trapping bolus increases in the upper half of the channel, while in the lower half, the size of the trapping bolus decreases with an increase of slip parameter β.

7) The number and size of the trapping bolus reduces in the upper half of the channel, while in the lower half, size of the trapping bolus increases with an increase of volume flow rate Q.

References

[1] CLMH Navier. Mémoire sur les lois du mouvement des fluids. *Mem. Acad. Sci. Inst. Fr.* 1827; **6**, 389-440.

[2] D Tripathi. Numerical study on creeping flow of Burgers' fluids through a peristaltic tube. *J. Fluid Eng.* 2011; **133**, 121104-9.

[3] MV Reddy, M Mishra, S Sreenadh and AR Rao. Influence of Lateral Walls on peristaltic flow in a rectangular duct. *J. Fluid Eng.* 2005; **127**, 824-7.

[4] MJ Miksis and SH Davis. Slip over rough and coated surface. *J. Fluid Mech*. 1994; **273**, 125-39.

[5] T Hayat, T Javed and Z Abbas. Slip flow and heat transfer of a second grade fluid past a stretching sheet through a porous space. *Int. J. Heat Mass Tran.* 2008; **51**, 4528-34.

[6] PD Ariel. Axisymmetric flow due to a stretching sheet with partial slip. *Comput. Math. Appl.* 2007; **54**, 1169-83.

[7] O Eytan, AJ Jaffa and D Elad. Peristaltic flow in a tapered channel: Application to embryo transport within the uterine cavity. *Med. Eng. Phys*. 2001; **23**, 473-82.

[8] MH Haroun. Effect of Deborah number and phase difference on peristaltic transport in an asymmetric channel. *Comm. Nonlinear Sci. Numer. Simulat.* 2007; **12**, 1464-80.

[9] TD Brown and TK Hung. Computational and experimental investigations of two dimensional non linear peristaltic flows. *J. Fluid Mech.* 1977; **83**, 249-72.

[10] AH Shapiro, MY Jaffrin and SL Weinberg. Peristaltic pumping with long wave length at low Reynolds number. *J. Fluid Mech.* 1969; **37**, 799-825.

[11] TW Latham. 1966, Fluid motion in a peristaltic pump. M. Sc. Thesis, Massachusetts Institute of Technology, Cambridge.

[12] AA Khan, R Ellahi and K Vafai. Peristaltic transport of Jeffrey fluid with variable viscosity through a porous medium in an asymmetric channel. *Adv. Math. Phys.* 2012; **2012**, 169642.

[13] S Nadeem, A Riaz and R Ellahi. Peristaltic flow of a Jeffrey fluid in a rectangular duct having compliant walls. *Chem. Ind. Chem. Eng. Q.* 2013; **19**, 399-409.

[14] R Ellahi, A Riaz and S Nadeem. Three dimensional peristaltic flow of Williamson in a rectangular duct. *Indian J. Phys.* 2013; **87**, 1275-81.

[15] KS Mekheimer. Effect of the induced magnetic field on peristaltic flow of a couple stress fluid.

Phys. Lett. A 2008; **372**, 4271-8.
[16] R Ellahi, A Riaz, S Nadeem and M Ali. Peristaltic flow of Carreau fluid in a rectangular duct through a porous medium. *Math. Probl. Eng.* 2012; **2012**, 329639.
[17] S Nadeem and S Akram. Heat transfer in a peristaltic flow of MHD fluid with partial slip. *Comm. Nonlinear Sci. Numer. Simulat.* 2010; **15**, 312-21.
[18] N Ali, Q Hussian, T Hayat and S Asghar. Slip effects on the peristaltic transport of MHD fluid with variable viscosity. *Phys. Lett. A* 2008; **372**, 1477-89.
[19] I Dapra and G Scarpi. Perturbation solution for pulsatile flow of a non-Newtonian Williamson fluid in a rock fracture. *Int. J. Rock Mech. Min. Sci*. 2007; **44**, 271-8.
[20] M Mishra and AR Rao. Peristaltic transport of a Newtonian fluid in an asymmetric channel. *Zeitschrift fur angewandte Mathematik and Physik* 2004; **54**, 532-50.